We are IntechOpen,
the world's leading publisher of
Open Access books
Built by scientists, for scientists

6,900
Open access books available

186,000
International authors and editors

200M
Downloads

154
Countries delivered to

Our authors are among the

TOP 1%
most cited scientists

12.2%
Contributors from top 500 universities

CLARIVATE ANALYTICS
BOOK CITATION INDEX
INDEXED

WEB OF SCIENCE™

Selection of our books indexed in the Book Citation Index
in Web of Science™ Core Collection (BKCI)

Interested in publishing with us?
Contact book.department@intechopen.com

Numbers displayed above are based on latest data collected.
For more information visit www.intechopen.com

Non-minutiae Based Fingerprint Descriptor

Jucheng Yang
School of information technology, Jiangxi University of Finance and Economics
Ahead Software Company Limited, Nanchang
China

1. Introduction

Fingerprint recognition refers to the techniques of identifying or verifying a match between human fingerprints. Fingerprint recognition has been one of the hot research areas in recent years, and it plays an important role in personal identification (Maio et al., 2003). A general fingerprint recognition system consists of some important steps, such as fingerprint pre-processing, feature extraction, matching, and so on. Usually, a descriptor is defined to identify an item with information storage. A fingerprint descriptor is used to descript and represent a fingerprint image for personal identification.

Various fingerprint descriptors have been proposed in the literature. Two main categories for fingerprint descriptors can be classified into minutiae based and non-minutiae based. Minutiae based descriptors (Jain et al. 1997a; Jain et al. 1997b; Liu et al. 2000; Ratha et al. 1996; He et al. 2007; Cappelli et al. 2011) are the most popular algorithms for fingerprint recognition and are sophisticatedly used in fingerprint recognition systems. The major minutia features of fingerprint ridges are: ridge ending, ridge bifurcation and so on (Maio et al., 2003). Minutiae based descriptor use a feature vector extracted from fingerprints as sets of points in a multi-dimensional space, which comprise several characteristics of minutiae such as type, position, orientation, etc. The matching is to essentially search for the best alignment between the template and the input minutiae sets. However, due to the poor image quality and complex input conditions, minutiae are not easy to be accurately determined, thus it may result in low matching accuracy. In addition, minutiae based descriptors may not fully utilize the rich discriminatory information available in the fingerprints with high computational complexity.

Non-minutiae based descriptors (Amornraksa & Tachaphetpiboon, 2006; Benhammadi, et al. 2007;Jain et al.,2000; Jin et al., 2004; Nanni and Lumini, 2008; Nanni & Lumini, 2009; Ross, et al. 2003; Sha et al. 2003；Tico et al. 2001; Yang et al., 2006; Yang & Park, 2008a; Yang & Park, 2008b), however, overcome the demerits of the minutiae based method. It uses features other than characteristics of minutiae from the fingerprint ridge pattern, such as local orientation and frequency, ridge shape, and texture information. It can extract more rich discriminatory information and abandon the pre-processing process such as binarization and thinning and post minutiae processing. Other merits are listed by using the non-minutiae based methods, such as a high accuracy; a fast processing speed; a fixed length feature vector; easily coupled with other system; being combined with Biohashing and so on.

Among various non-minutiae based descriptors, Gabor feature-based ones (Jain et al.,2000; Sha et al. 2003) present a relatively high matching accuracy by using a bank of Gabor filters to capture both the local and global details in a fingerprint, and represent them as a compact fixed-length fingerCode. Ross et al. (2003) describes a hybrid fingerprint descriptor that uses both minutiae and a ridge feature map constructed by a set of eight Gabor filters. Benhammadi et al. (2007) also propose a new hybrid fingerprint descriptor based on minutiae texture maps according to their orientations. It exploits the eight fixed directions of Gabor filters to generate its weighting oriented Minutiae Codes. Tico et al. (2001) propose a transform-based descriptor using digital wavelet transform (DWT) features. The features are obtained from the standard deviations of the DWT coefficients of the image details at different scales and orientations. Amornraksa & Tachaphetpiboon (2006) propose another transform-based descriptor using digital cosine transform (DCT) features. The transform methods show a high matching accuracy for inputs identical to one in its database. Jin et al. (2004) propose an improved transform-based descriptor based on the features extracted from the integrated wavelet and Fourier-Mellin transform (WFMT) framework. Multiple WFMT features can be used to form a reference invariant feature through the linearity property of FMT and hence to reduce the variability of the input fingerprint images. Nanni & Lumini (2008) proposed a hybrid fingerprint descriptor based on local binary pattern (LBP). Nanni & Lumini (2009) proposed another descriptor based on histogram of oriented gradients (HoG). Yang et al. (2006) propose a fingerprint descriptor using invariant moments (IM) with the learning vector quantization neural network (LVQNN) for matching, which use a fixed-size ROI (Region of Interest) to extract seven invariant moments as a feature vector. Its improved ones (Yang & Park, 2008a; Yang & Park, 2008b;) using tessellated invariant moments(Tessellated IM) or sub-regions IM with eigenvalue-weighted cosine (EWC) distance or nonlinear back-propagation Neural Networks (BPNN) to handle the various input conditions for fingerprint recognition.

In this chapter, some state of the art non-minutiae based descriptors are first reviewed, and a non-minutiae based fingerprint descriptor with tessellated invariant moment features, feature selection with PCA (Principle Component Analysis), and a Support Vector Machine (SVM) for classification is proposed. The proposed descriptor basically uses moment features invariant to scale, position and rotation to increase the matching accuracy with a low computational load. It further pursues an improved performance by using the alignment and rotation after a sophisticated, reliable detection of a reference point. Having invariant characteristics in the proposed algorithm can significantly improve the performance for input images under various conditions. To fully utilize both the global and local ridge information while removing unwanted noises, the algorithm extracts features from tessellated cells around the reference point. Combining with the PCA for feature selection to reduce the dimension of feature vector and choose the distinct features. Matching with a SVM also contributes to the performance enhancement by simply assigning weights on different cells and classification with high accuracy.

The chapter is organized as follows: some state of the art non-minutiae based descriptors are briefly reviewed in section 2. In section 3, a proposed non-minutiae based fingerprint descriptor with tessellated invariant moments and SVM is explained. And experimental results are illuminated in section 4. Finally, conclusion remarks are given in section 5.

2. Non-minutiae based descriptors

It is important to establish descriptors to extract reliable, independent and discriminate fingerprint image features. Exception of the widely used minutiae descriptors, the non-minutiae based descriptors use features other than characteristics of minutiae from the fingerprint ridge pattern are able to achieve the characters of the mentioned fine traits . The features of these descriptors may be extracted more reliably than those of minutiae. The next sub-sections will introduce some classical and state of the art non-minutiae based descriptors, such as Gabor filters, DWT, DCT, WFMT, LBP, HOG, IM based.

2.1 Gabor filters based descriptor

The Gabor filters based descriptors (Jain et al.,2000; Sha et al. 2003) have been proved with their effectiveness to capture the local ridge characteristics with both frequency-selective and orientation-selective properties in both spatial and frequency domains. They describe a new texture descriptor scheme called fingerCode which is to utilize both global and local ridge descriptions to represent a fingerprint image. The features are extracted by tessellating the image around a reference point (the core point) determined in advance. The feature vector consists of an ordered collection of texture descriptors from some tessellated cells. Since the scheme assumes that the fingerprint is vertically oriented, to achieve invariance, image rotation is compensated by computing the features at various orientations. The texture descriptors are obtained by filtering each sector with 8 oriented Gabor filters and then computing the AAD (Average Absolute Deviation) of the pixel values in each cell. The features are concatenated to obtain the fingerCode. Fingerprint matching is based on finding the Euclidean distance between the two corresponding FingerCodes.

However, the Gabor filters based descriptors are not rotation invariant. To achieve approximate rotation invariance, each fingerprint has to be represented with ten associated templates stored in the database, and the template with the minimum score is considered as the rotated version of the input fingerprint image. So these methods require a larger storage space and a significantly high processing time.

Recently, some hybrid descriptors combined with Gabor filters are proposed. Ross et al. (2003) describes a hybrid fingerprint descriptor that uses both minutiae and a ridge feature map constructed by a set of eight Gabor filters. The ridge feature map along with the minutiae set of a fingerprint image is used for matching purposes. The hybrid matcher is proved to perform better than a minutiae-based fingerprint matching system by the author.

Benhammadi et al. (2007) also propose a hybrid fingerprint descriptor based on minutiae texture maps according to their orientations. Rather than exploiting the eight fixed directions of Gabor filters for all original fingerprint images filtering process, they construct absolute images starting from the minutiae localizations and orientations to generate the Weighting Oriented Minutiae Codes. The extracted features are invariant to translation and rotation, which avoids the fingerprint pair relative alignment stage.

Another Gabor filters based descriptor is proposed by Nanni & Lumini (2007), where the minutiae are used to align the images and a multi-resolution analysis performed on separate regions or sub-windows of the fingerprint pattern is adopted for feature extraction and classification. The features extracted are the standard deviation of the image convolved with 16 Gabor filters. The similarity measurement is done by the weighed Euclidean distance matchers with a sequential forward floating scheme.

However, the matching accuracy of these hybrid approaches may be degraded for low-quality inputs, since the performance highly depends on extracting all minutiae precisely and reliably.

2.2 DWT based descriptor

Tico et al. (2001) proposed a method using DWT features. The features are obtained from the standard deviations of the DWT coefficients of the entire image details at different scales and orientations to form a feature vector of length 12 (48 in total from four subimages). The normalized l_2-norm of each wavelet sub-image is computed in order to create a feature vector. The feature vector represents an approximation of the image energy distribution. Fingerprint matching is based on k-Nearest Neighbor (KNN) with finding the Euclidean distance between the corresponding feature vectors.

However, the features extraction from frequency domain with corresponding transforms are not rotation-invariant, so if the image input with rotation, the features from the same fingerprint image can be judged into the different ones.

2.3 DCT based descriptor

Amornraksa & Tachaphetpiboon (2006) also propose a method using digital cosine transform (DCT) features for fingerprint matching. The standard deviations of the DCT coefficients located in six predefined areas from a 64×64 ROI are used as a feature vector of length 6 (24 in total from four sub-images) for fingerprint matching.

To extract the informative features from a fingerprint image, the image is first cropped to a 64×64 pixel region, centred at the reference point, and then quartered to obtain four non-overlapping sub-images of size 32×32 pixels. Next, the DCT is applied to each sub-image to obtain a block of 32×32 DCT coefficients. Finally, the standard deviations of the DCT coefficients located in six predefined areas are calculated and used as a feature vector of length 6 (24 in total from four sub-images) for fingerprint matching. Fingerprint matching is also based on KNN with the Euclidean distance.

However, the features are not rotation-invariant, too, to achieve rotation-invariant, so an improved method needs.

2.4 Integrated wavelet and the Fourier–Mellin transform (WFMT) based descriptor

Jin et al. (2004) propose an improved transform-based descriptor extracted features from the integrated wavelet and Fourier-Mellin transform (WFMT) framework. Wavelet transform, with its energy compacted feature is used to preserve the local edges and reduce noise in the low frequency domain, is able to make the fingerprint images less sensitive to shape distortion. The Fourier–Mellin transform (FMT) serves to produce a translation, rotation and scale invariant feature. And multiple WFMT features can be used to form a reference invariant feature through the linearity property of FMT and hence reduce the variability of the input fingerprint images. Multiple m WFMT features can be used to form a reference WFMT feature and just only one representation per user needs to be stored in the database. Fingerprint matching is based on finding the Euclidean distance between the corresponding multiple WFMT feature vectors.

However, the main disadvantage of this descriptor is that the reference point is based on a non-precise core point, and the descriptor requires a high time-consuming process if using the multiple WFMT features with training images.

2.5 Local binary pattern (LBP) based descriptor

Nanni & Lumini (2008) proposed a fingerprint descriptor based on LBPs. A LBP proposed by Ojala et al. (2002) is a grayscale local texture operator with powerful discrimination and low computational complexity. Moreover, it is invariant to monotonic grayscale transformation, hence the LBP representation may be less sensitive to changes in illumination. The two fingerprints to be matched are first aligned using their minutiae, then the images are decomposed in several overlapping sub-windows; and a Gabor filter with LBP hybrid method (GLBP) also proposed by Nanni & Lumini (2008), instead of from the original sub-windows, each sub-window is convolved with a bank of Gabor filters and the invariant LBPs histograms are extracted from the convolved images. The matching value between two fingerprint images is performed by a complex distance function that takes into account the presence of different types of descriptors and different regions.

However, the matching accuracy depends on extracting all minutiae precisely and reliably, and it may be degraded for low-quality inputs.

2.6 Histogram of oriented gradients (HoG) based descriptor

Nanni & Lumini (2009) recently proposed a hybrid fingerprint descriptor based on HoG. HoG has been first proposed by Dalal & Triggs (2005) as an image descriptor for localizing pedestrians in complex images and has reached increasingly popularity. The aim of this descriptor is to represent an image by a set of local histograms which count occurrences of gradient orientation in a local cell of the image. The implementation of the HoG descriptors can be achieved by computing gradients of the image; dividing the image into small sub-regions; building a histogram of gradient directions and normalizing histograms within some groups of sub-regions for each sub-region to achieve a better invariance to changes in illumination or shadowing. The matching value between two fingerprint images is performed by a complex distance function, too.

However, similar with the above minutiae based alignment methods, the matching accuracy depends on extracting all minutiae precisely and reliably.

2.7 IM based descriptor

Except for the above non-minutiae based descriptor, recently, Yang et al. (2006) propose an IM based descriptor with the LVQNN for fingerprint matching, which use a fixed-size ROI to extract seven invariant moments as a feature vector. And its improved ones (Yang & Park, 2008a; Yang & Park, 2008b;) using tessellated IM or sub-regions IM with EWC distance or nonlinear BPNN to handle the various input conditions for fingerprint recognition. The details of the invariant moments are introduced as below:

2.7.1 Raw moments

For a 2-dimensional continuous function f(x,y) the moment (sometimes called 'raw moment') of order (p + q) is defined as

$$m_{pq} = \int\limits_{-\infty}^{\infty} \int\limits_{-\infty}^{\infty} x^p y^q f(x,y) dx dy \tag{1}$$

for p, q= 0, 1, 2,…

Adapting this to scalar (grey-tone) image with pixel intensities I(x,y), raw image moments are calculated by

$$m_{pq} = \sum_x \sum_y x^p y^q I(x,y) \tag{2}$$

In some cases, this may be calculated by considering the image as a probability density function, i.e., by dividing the above by

$$\sum_x \sum_y I(x,y) \tag{3}$$

A uniqueness theorem (Papoulis, 1991) states that if f(x,y) is piecewise continuous and has nonzero values only in a finite part of the xy plane, moments of all orders exist, and the moment sequence (Mpq) is uniquely determined by f(x,y). Conversely, (Mpq) uniquely determines f(x,y). In practice, the image is summarized with functions of a few lower order moments.

Simple image properties derived via raw moments include:

1.   Area (for binary images) or sum of grey level (for grey-tone images):
The Area (A) of the image can be extracted by the formula:

$$A = m_{00} \tag{4}$$

2.   Centroid point of the image:
The centroid point $\{\bar{x}, \bar{y}\}$ of the image can be extracted by the formula:

$$\{\bar{x}, \bar{y}\} = \{m_{10}/m_{00}, m_{01}/m_{00}\} \tag{5}$$

2.7.2 Central moments

a.   The central moments are defined as

$$\mu_{pq} = \int_{-\infty}^{\infty} \int_{-\infty}^{\infty} (x - \bar{x})^p (y - \bar{y})^q f(x,y) dx dy \tag{6}$$

Where

$$\bar{x} = m_{10}/m_{00} \quad and \quad \bar{y} = m_{01}/m_{00} \tag{7}$$

If f(x,y) is a digital image, then Eq.(6) becomes

$$\mu_{pq} = \sum_x \sum_y (x - \bar{x})^p (y - \bar{y})^q f(x,y) \tag{8}$$

b.   The meanings of the central moments are listed as below:

1. μ_{20} represents he horizontal extension parameter of the image;
2. μ_{02} represents vertical extension of the image;
3. μ_{11} represents the gradient of the image, if $\mu_{11} > 0$,it means the image inclines towards up-left; if $\mu_{11} < 0$,it means the image inclines towards up-right;

4. μ_{30} represents the excursion degree of the image's barycenter on horizontal direction, when $\mu_{30} > 0$, the barycenter inclines towards left; then if $\mu_{30} < 0$, the barycenter inclines towards right ;

5. μ_{03} represents the vertical excursion degree of the image's barycenter, if $\mu_{03} > 0$, the barycenter inclines towards upward, and inclines towards downward while $\mu_{03} < 0$;

6. μ_{21} represents the equilibrium degree about the image on the vertical direction, if $\mu_{21} > 0$, the extension of the downside image is greater than the upside; then smaller when $\mu_{21} < 0$;

7. μ_{12} represents the equilibrium degree of the image about the vertical direction, when $\mu_{12} > 0$, the image's extension on the right side is greater than the left side, then smaller when $\mu_{12} < 0$.

c. Normalized moments:

Moments where p+q >=2 can also be invariant to both translation and changes in scale by dividing central moments by the properly scaled μ_{00} moment, as the normalized central moments, denoted η_{pq} , are defined as

$$\eta_{pq} = \frac{\mu_{pq}}{\mu_{00}^{\gamma}} \tag{9}$$

where $\gamma = \frac{p+q}{2} + 1$ for p+q = 2, 3...

2.7.3 Invariant moments

As a region description method, invariant moments are used for texture analysis and pattern identification. A set of seven invariant moments derived from the second and the third moments were proposed by Hu (1962). As the equation shown below, Hu derived the expressions from algebraic invariants applied to the moment generating function under a rotation transformation. The set of moment invariants consist of groups of nonlinear centralized moment expressions. And they are scale, position, and rotation invariant (Gonzalez and woods, 2002).

$$
\begin{aligned}
\phi_1 &= \eta_{20} + \eta_{02} \\
\phi_2 &= (\eta_{20} - \eta_{02})^2 + 4\eta_{11}^2 \\
\phi_3 &= (\eta_{30} - 3\eta_{12})^2 + (3\eta_{21} - 3\eta_{03})^2 \\
\phi_4 &= (\eta_{30} + \eta_{12})^2 + (\eta_{21} + \eta_{03})^2 \\
\phi_5 &= (\eta_{30} - 3\eta_{12})(\eta_{30} + \eta_{12})[(\eta_{30} + \eta_{12})^2 - 3(\eta_{21} + \eta_{03})^2] \\
&\quad + (3\eta_{21} - \eta_{03})(\eta_{21} + \eta_{03})[3(\eta_{30} + \eta_{12})^2 - (\eta_{21} + \eta_{03})^2] \\
\phi_6 &= (\eta_{20} - \eta_{02})(\eta_{30} + \eta_{12})[(\eta_{30} + \eta_{12})^2 - (\eta_{21} + \eta_{03})^2] \\
&\quad + 4\eta_{11}(\eta_{30} + \eta_{12})(\eta_{21} + \eta_{03}) \\
\phi_7 &= (3\eta_{21} - \eta_{03})(\eta_{30} + \eta_{12})[(\eta_{30} + \eta_{12})^2 - 3(\eta_{21} + \eta_{03})^2] \\
&\quad + (3\eta_{12} - \eta_{30})(\eta_{21} + \eta_{03})[3(\eta_{30} + \eta_{12})^2 - (\eta_{21} + \eta_{03})^2]
\end{aligned}
\tag{10}
$$

The values of the computed moment invariants are usually small values of higher order moment invariants are close to zero in some cases. So we reset the value range using the logarithmic function, the outputs of the moment invariants are mapped into $\Phi_i = |\lg(|\phi_i|)|$ $i=1,2,...7$, which can take the values to the large dynamic range with a nonlinear scale.

Figure 1 and Figure 2 show the invariant moments analysis on the four sub-images with 2D and 3D views, respectively. The experiments here are designed to check the characteristics of the invariant moment features' invariance to rotation and scale. We choose four sub-images from a ROI of a fingerprint image, and divide the ROI into four sub-images. From the figures, we can see that the ridge valleys of the sub-images are totally different.
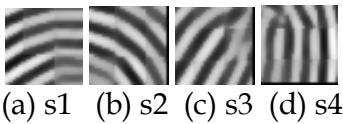
(a) s1   (b) s2   (c) s3   (d) s4

Fig. 1. Sub-images of sub-images (a) s1 (b) s2 (c) s3 (d) s4

(a) s1   (b) s2

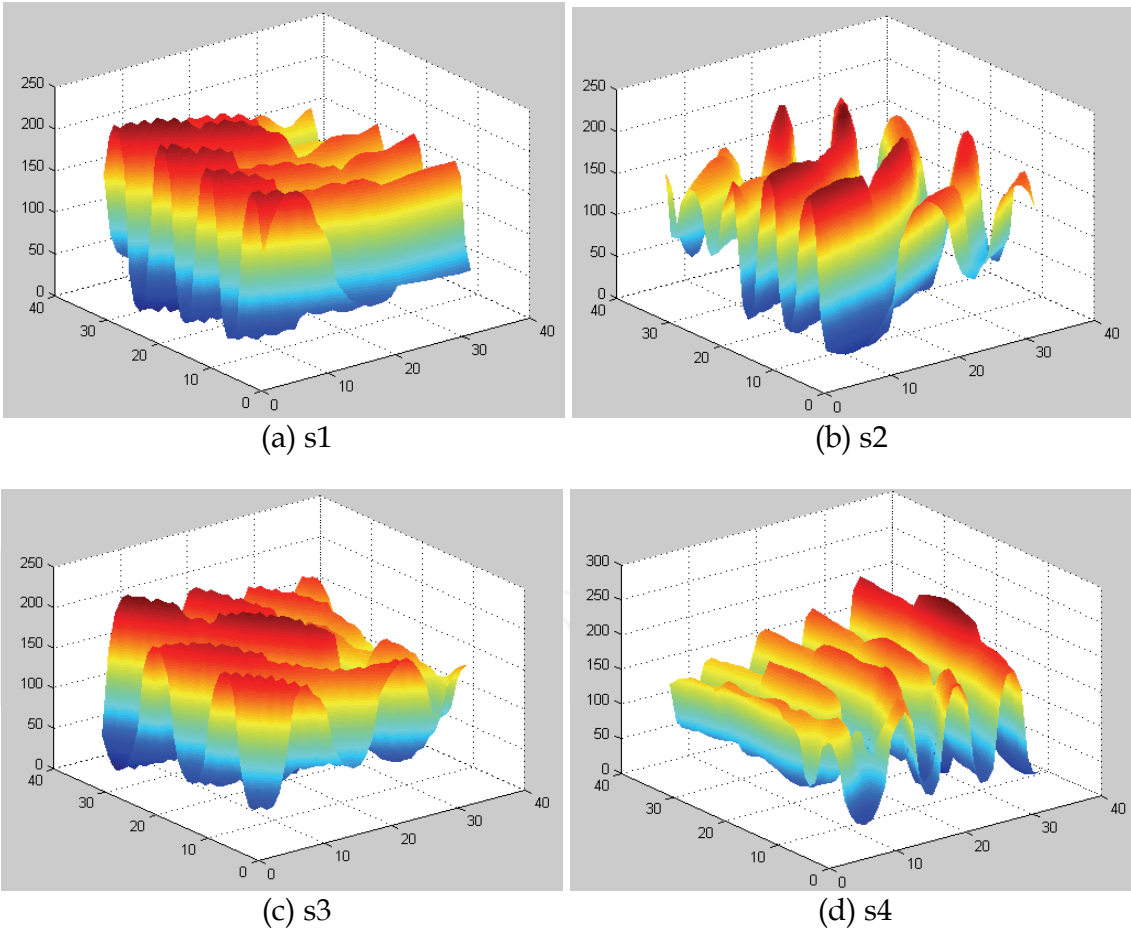(c) s3   (d) s4

Fig. 2. 3D images of sub-images (a) s1 (b) s2(c) s3 (d) s4

And Table 1 and Table 2 show seven invariant moments of these four sub-images, and scale, rotation invariance of sub-image S1, respectively. As we can see from the tables, the invariant moments are nearly invariant to the scale and rotation invariance.

Sub-image	Φ_1	Φ_2	Φ_3	Φ_4	Φ_5	Φ_6	Φ_7
S1	6.660157	22.792705	27.607114	29.742121	59.753254	41.222497	58.474584
S2	6.664572	20.127298	29.650909	29.742485	59.945926	39.811898	59.811871
S3	6.676695	21.271717	28.456694	29.916016	60.753962	41.309514	59.528609
S4	6.674009	20.209754	28.826501	29.101012	58.682184	39.417999	58.701581

Table 1. Seven invariant moments of the four sub-images

Scale	Rotation	Φ_1	Φ_2	Φ_3	Φ_4	Φ_5	Φ_6	Φ_7
0.8	0	6.659508	21.450452	27.459971	30.169709	59.518255	41.693181	59.301135
	90	6.657605	21.641931	27.433996	31.337310	63.211065	43.918130	61.111226
	180	6.657625	21.654452	27.376333	31.318065	61.275622	42.931670	60.714937
	270	6.659334	21.473568	27.400168	30.162576	60.756198	41.433472	59.053503
1	0	6.660157	22.792705	27.607114	29.742121	59.753254	41.222497	58.474584
	90	6.660157	22.792705	27.607114	29.742121	58.901367	41.222497	58.474584
	180	6.660157	22.792705	27.607114	29.742121	59.753254	41.222497	58.474584
	270	6.660157	22.792705	27.607114	29.742121	58.901367	41.222497	58.474584
2	0	6.659431	22.792705	27.607114	29.742121	59.753254	41.222497	58.474584
	90	6.659431	22.792705	27.607114	29.742121	58.901367	41.222497	58.474584
	180	6.659431	22.792705	27.607114	29.742121	59.753254	41.222497	58.474584
	270	6.659431	22.792705	27.607114	29.742121	58.901367	41.222497	58.474584

Table 2. Scale, rotation invariance of sub-image S1

2.8 Tessellated invariant moments based descriptors

In order to reduce the effects of noise and non-linear distortions, and speed up the processing time, tessellated IM based descriptors (Yang & Park, 2008a) using only a certain area (ROI) around the reference point at the centre as the feature extraction area instead of using the entire fingerprint is proposed. By adjusting the size of ROI and the number of the cells, we can capture both the local and global structure information around the reference point (see Figure 3 (a-b)). The ROI is partitioned into some non-overlapping rectangular cells as depicted in Figure 3 (a), e.g. the size of ROI is 64×64 pixels, 16 rectangular cells, and each cell has a size of 16×16 pixels.

Invariant moment analysis introduced in section 2 is used as the features for the fingerprint recognition system. For each cell, a set of seven invariant moments are computed. Suppose $\phi = \{\phi_n\}_{n=1}^7$ is a set of invariant moments, and $s = \{s_n\}_{n=1}^N$ is the collection of all the cells,

$$s = \{s_n\}_{n=1}^N = \{\{\phi_{nk}\}_{k=1}^7\}_{n=1}^M \tag{11}$$

where M is the number of the cells, N=7M is the total length of the collection.

Furthermore, in order to improve the matching accuracy, weights w is assigned to each tessellated cell to distinguish the cell from the foreground or background, which can be used to resolve the embarrassment when the reference point is nearby the border of the

fingerprint image. If the tessellated cells that contain a certain proportion of the background pixels, it will be labelled as background cells and the corresponding w is set to 0, else w equals 1. Therefore, a fingerprint can be represented by a fixed-length feature vector as

$$f = \{f_n\}_{n=1}^N = \{ws_n\}_{n=1}^N \tag{12}$$
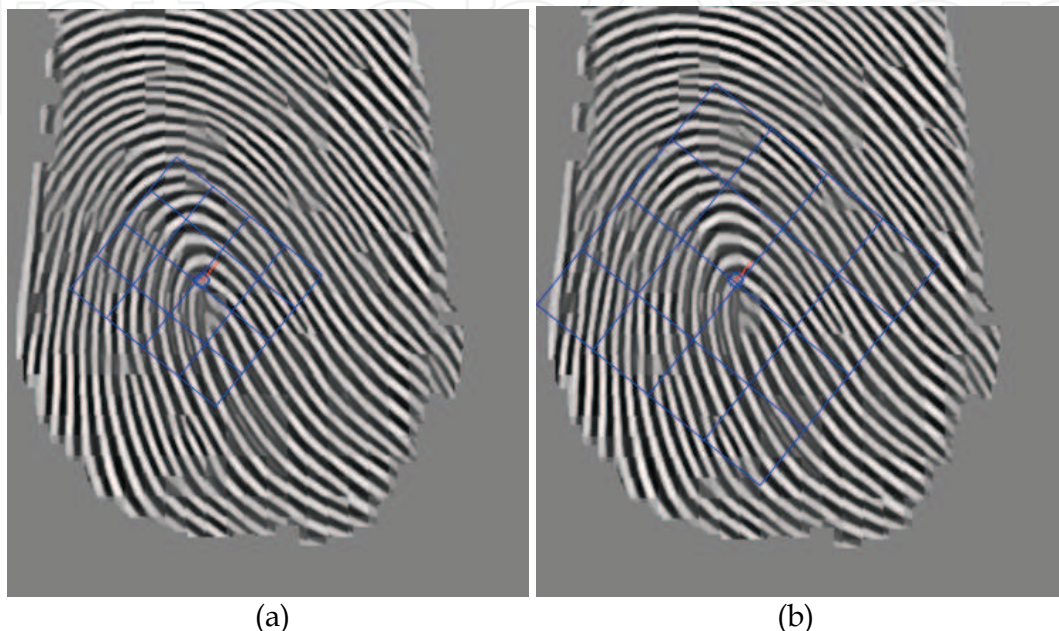
The length of the total feature vectors is N.

(a)   (b)

Fig. 3. (a) Tessellated cells (local) or (b) tessellated cells (global) (Yang & Park, 2008a)

2.9 Summarization

As the above analysis, all kinds of non-minutiae descriptor has proposed to hand the shortcomings of minutiae methods in the fingerprint recognition systems. Table 3 gives a summarization of some classical and state-of-art non-minutiae based descriptors in these recent years, such as Gabor filters, DWT, DCT, WFMT, LBP, HOG, IM based, and analyzes their feature extraction, alignment, and matching methods.

Table 3 summarizes the classical and state of the art non-minutiae based method (EER is the equal error rate, FAR is the false acceptance rate, FRR is the false reject rate, and GAR is the genuine acceptance rate (GAR = 1-FRR)). From the table, we can see that based on the public database of FVC2002 DB2, the sub-regions IM method with BPNN has the lowest EER of 3.26%, which means its performance is the best among all the non-minutiae descriptors on the same public database listed in the table.

3. Proposed non-minutiae based descriptor

Although the IM descriptor proposed in Yang & Park (2008a) and Yang & Park (2008b) use the tessellated or sub-regions IM to extract both the local and global features, comparing to Yang et al. (2006) just using only a fixed ROI, the tessellated or sub-regions ROIs are delineated from the same area of a fingerprint image, strong correlation may exist among the extracted features, and the dimension of the features are high. An improvement way is

proposed here to reduce the dimension of feature vector and choose the distinct features before matching.

PCA is one of the oldest and best known techniques in multivariate analysis (Fausett, 1994). So we reduce the dimension of feature vector by examining feature covariance matrix and then selecting the most distinct features and using them to improve the verification performance. Besides, as a powerful classification tool, a SVM is proposed for fingerprint matching.

Approaches	Features	Alignment methods	Matching methods	Performance analysis	
				Databases	Resutls
Jain et al.(2000)	Gabor filters	Core point	Euclidean distance	Self	FAR=4.5 FRR=2.8
Ross et al. (2003)	Gabor filters& Minutiae	Minutiae	Euclidean distance	Self	EER=4
Benhammadi et al. (2007)	Minutiae Gabor filters maps	Minutiae	Normalized distance	FVC2002 DB2	EER=5.19
Nanni & Lumini (2007)	Gabor filters	Minutiae	Weighed Euclidean distance	FVC2002 DB 2	EER=3.6
Tico et al. (2001)	DWT	NO	KNN with Euclidean distance	Self &small	Recognition rates 95.2
Amornraksa & Tachaphetpiboon (2006)	DCT	NO	KNN with Euclidean distance	Self &small	Recognition rates 99.23
Jin et al. (2004)	WFMT	Core point	Euclidean distance	FVC2002 DB 2	EER=5.309
Nanni & Lumini (2008)	LBP	Minutiae	Complex distance function	FVC2002 Db2	EER=6.2
Nanni & Lumini (2009)	HoG	Minutiae	Complex distance function	FVC2002 DB 2	EER=3.8
Yang et al. (2006)	Seven IM	Reference point	LVQNN	FVC2002 DB 2	FAR=0.6G AR=96.1
Yang & Park (2008a)	Tessellated IM	Reference point	EWC distance	FVC2002 DB 2	EER=3.78
Yang & Park (2008b)	Sub-regions IM	Reference point	BPNN	FVC2002 DB 2	EER=3.26

Table 3. Summarization of the classical and state of the art non-minutiae based method

3.1 Feature vector construction
After the pre-processing steps of fingerprint enhancement, reference point determination and image alignment, ROI determination (Yang & Park, 2008a; Yang & Park, 2008b; Yang et

al, 2008c), due to the good characteristics of reducing the effects of noise and non-linear distortions, we use the tessellated IM as the features, and a fingerprint can be represented by a fixed-length feature vector as $f = \{f_n\}_{n=1}^{N} = \{ws_n\}_{n=1}^{N} = \left\{w\{\phi_{nk}\}_{k=1}^{7}\right\}_{n=1}^{N}$, as descript in section 2.8, where $\phi = \{\phi_n\}_{n=1}^{7}$ is a set of invariant moments, and the length of the total feature vectors is N, w is the weight of distinguishing the cell from the foreground or background. For example, the ROI is partitioned into some non-overlapping rectangular cells with the size of ROI is 64×64 pixels, 16 rectangular cells, and each cell has a size of 16×16 pixels. Then the feature-vector with the elements consists of a sets of moments derived from tessellated ROIs. So the total length of the feature vector is 16x7=112.

3.2 Feature selection with PCA

Here, the feature selection with PCA is briefly introduced. The objective of PCA is to reduce the dimensionality of the data set, while retaining as much as possible variation in the data set, and to identify new meaningful underlying variables.

The basic idea in PCA is to find the orthonormal features. Let x ∈ Rn be a random vector, where n is the dimension of the input space. The first principal component is the projection in the direction in which the variance of the projection is maximized. The mth principal component is determined as the principal component of the residual based on the covariance matrix.

The covariance matrix of x is defined as Ξ = E{[x-E(x)][x-E(x)]^T}. Let u1, u2, . . . , un and λ1, λ2, . . . , λn be eigenvectors and eigenvalues of Ξ, respectively, and λ1 ≥ λ2 ≥. . . ≥ λn.

Then, PCA factorizes Ξ into Ξ = UΛU^T, with U = [u1, u2, . . . , un] and Λ = diag(λ1, λ2, . . . , λn). We need to note that once the PCA of Ξ is available, the best rank-m approximation of Ξ can be readily computed.

Let P = [u1, u2, . . . , um], where m < n. Then y = P^{T}x will be an important application of PCA in dimensionality reduction.

3.3 Matching with SVM

SVMs (John & Nello, 2000) are a set of related supervised learning methods used for classification and regression. Viewing input data as two sets of vectors in an n-dimensional space, a SVM will construct a separating hyperplane in that space, one which maximizes the margin between the two data sets. To calculate the margin, two parallel hyperplanes are constructed, one on each side of the separating hyperplane, which are 'pushed up against' the two data sets. Intuitively, a good separation is achieved by the hyperplane that has the largest distance to the neighboring data points of both classes, since in general the larger the margin the better the generalization error of the classifier.

SVM is a powerful tool for solving small sample learning problem that offers favorable performance using linear or nonlinear function estimators. It is a type of neural network that automatically determines the structural components. In our study, we used a two-class SVM to classify the input fingerpints into the corresponding class. Let the training set be $\left\{(\mathbf{x}_i, y_i)\right\}_{i=1}^{m}$, with input vector $\mathbf{x}_i$ (n components), $y_i = \pm 1$ indicates two different classes and $i = 1, 2, ..., m$. The decision function of SVM is:

$$y = sign(\sum_{i=1}^{m} \alpha_i y_i K(\mathbf{x}_i, \mathbf{x}) + b) = sign(\sum_{i=1}^{m} \omega_i K(\mathbf{x}_i, \mathbf{x}) + b) \tag{13}$$
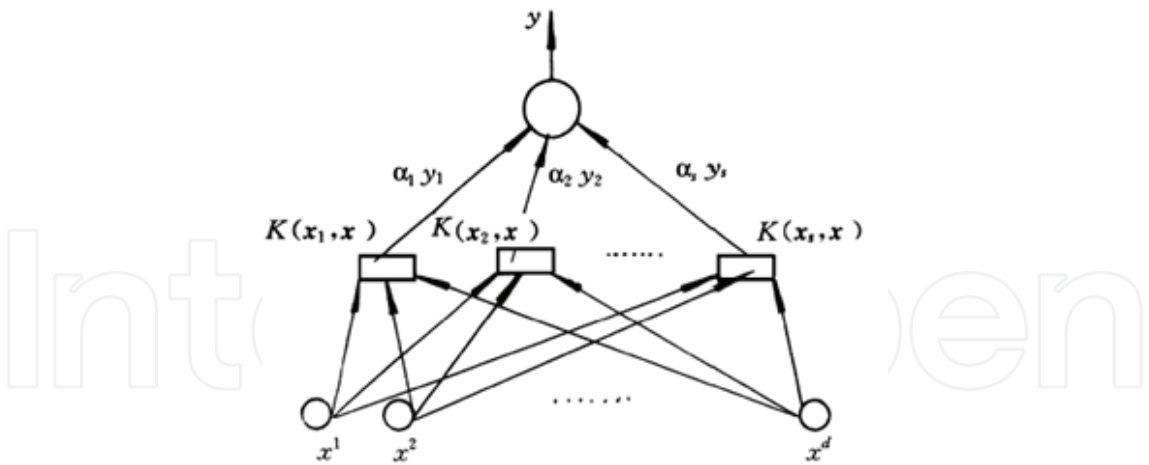
Fig. 4. Illustration of a SVM structure

Figure 4 illustrates the structure of a SVM, where $K(\mathbf{x}_i,\mathbf{x})$ is the output of the ith hidden node with respect to the input vector $\mathbf{x}$, it is a mapping of the input $\mathbf{x}$ and the support vector $\mathbf{x}_i$ in an alternative space (the so-called feature space), by choosing the kernel $K(\mathbf{x}_i,\mathbf{x}) = \phi(\mathbf{x}_i) \cdot \phi(\mathbf{x})$. α_i and b are the learning parameters of the hidden nodes, and $\omega_i = \alpha_i y_i$ is the weight of the ith hidden node connecting with the output node. The learning task of a SVM is to find the optimal α_i by solving the maximization of the Lagrangian

$$W(\alpha) = \sum_{i=1}^{m}\alpha_i - \frac{1}{2}\sum_{i,j=1}^{m}\alpha_i\alpha_j y_i y_j K(\mathbf{x}_i,\mathbf{x}_j) \tag{14}$$

subject to the constraints

$$\sum_{i=1}^{m}\alpha_i y_i = 0 \qquad 0 \le \alpha_i \le c \tag{15}$$

The common kernel functions $K(\mathbf{x}_i,\mathbf{x})$ are defined as :

$$K(\mathbf{x}_i,\mathbf{x}) = \begin{cases} \mathbf{x}_i^T \cdot \mathbf{x} & Linear \\ (\gamma \cdot \mathbf{x}_i^T \cdot \mathbf{x} + c)^{Degree} & Polynomial \\ \exp(-\gamma \cdot \left\|\mathbf{x}_i - \mathbf{x}\right\|^2) & Radial-basis \\ \tanh(\gamma \cdot \mathbf{x}_i^T \cdot \mathbf{x} + c) & Sigmoid \end{cases} \tag{16}$$

Where γ ,c ,Degree are the kernel parameters.

4. Experimental results

The proposed algorithm was evaluated on the fingerprint images taken from the public FVC2002 database (Maio et al. 2002), which contains 4 distinctive databases: DB1_a, DB2_a, DB3_a and DB4_a. The resolution of DB1_a, DB3_a, and DB4_a is 500 dpi, and that of DB2_a is 569 dpi. Each database consists of 800 fingerprint images in 256 gray scale levels (100 persons, 8 fingerprints per person). Fingerprints from 101 to 110 (set B) have been made available to the participants to allow parameter tuning before the submission of the

algorithms; the benchmark is then constituted by fingers numbered from 1 to 100 (set A). In our experiments, the used FVC2002databases are set A.

4.1 Performances with a SVM matching

In the experiments, a SVM is used to verify a matching between feature vectors of input fingerprint and those of template fingerprint, the number of the output class is the same with the verifying persons. For each input fingerprint and its template fingerprint, we compute the IM features. Since the output is to judge whether the input fingerprint is match or non-match according to the identity ID, we can take the matching process as a two-class problem.

In the training stage, training samples after normalization and scale processing (Hao, et al. 2007) are fed to a SVM with indicating their corresponding class. The features are computed from the training data, each contains vector from the training fingerprint, and the identity ID of the corresponding class is used to guide the classifying results through the SVM. While in the testing stage, test samples with the same normalization and scale processing are fed to the SVM to produce the output values. Similarly, the features are computed from the testing data, each contains vector from the test fingerprint with the corresponding identity ID. The element of the output values is restricted in the class number. If the output number is equal the corresponding ID, then it means match, vice visa.

To evaluate the performance of the verification rate of the proposed method, the receiver operating characteristic (ROC) curve is used. An ROC curve is a plot of false reject rate (FRR) against false acceptance rate (FAR). The FRR and FAR are defined as follows:

$$FRR = \frac{\text{Number of rejected genuine claims}}{\text{Total number of genuine accesses}} \times 100\% \tag{17}$$

$$FAR = \frac{\text{Number of accepted imposter claims}}{\text{Total number of imposter accesses}} \times 100\% \tag{18}$$

The equal error rate (EER) is also used as a performance indicator. The EER indicates the point where the FRR and FAR are equal, as below.

$$EER = (FAR + FRR)/2, \ \text{if} \ FAR = FRR \tag{19}$$

For evaluating the recognition rate performance of the proposed descriptor, we did experiments on FVC2002 databases DB2_a. We divided the database into a training set and a testing set. Six out of eight fingerprints from each person were chosen for training and all the eight fingerprints for testing. For a database, therefore, 600 patterns were used for training, and 800 for testing. In the experiments, the 64×64 pixels size of ROI was adopted, and the ROI was tessellated into 16 rectangular cells with each cell had a size of 16×16 pixels. So the length of the feature vector was 16×7=112. In the feature selection experiments, the feature-vector with the elements consisting of a sets of moments derived from tessellated ROIs was processed with PCA. The new dimensional features are uncorrelated from original features due to the PCA analysis. Figure 5 describes the egienvalues spectrum with different elements by using PCA for feature selection. Since our feature vector contains 112 elements, from the figure, we can see that almost all the egienvalues spectrum with the eigenvectors elements are below than 70, if we keep 95% energy, then eigenvectors element of 50 was chosen.
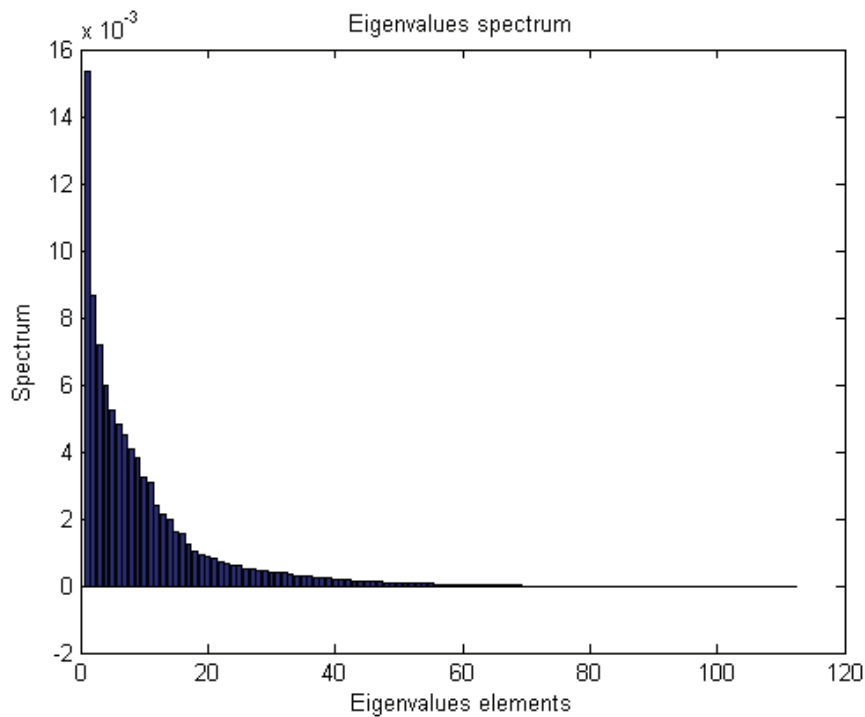
Fig. 5. The egienvalues spectrum with different elements by using PCA for feature selection
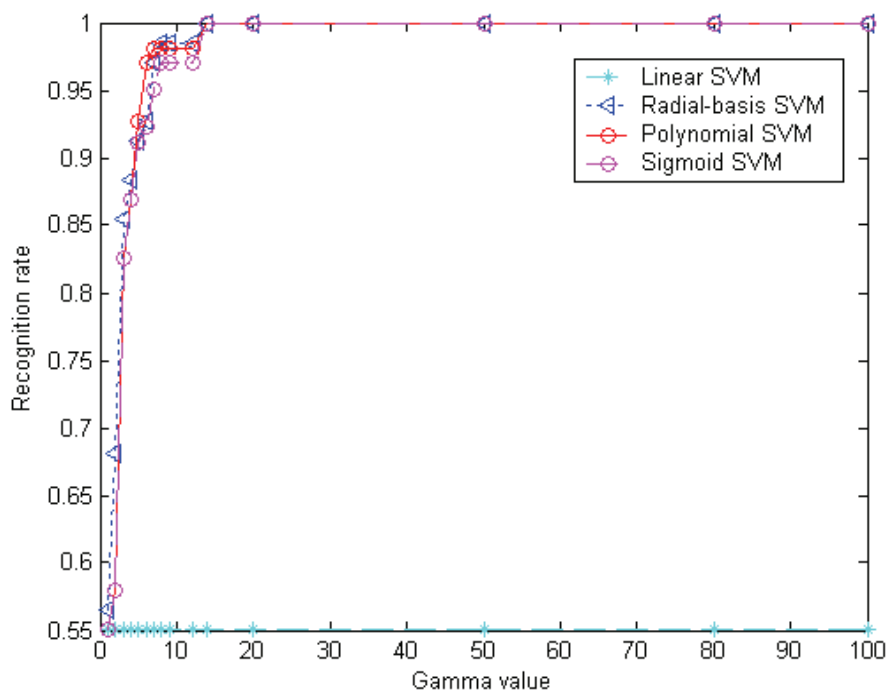

Fig. 6. The curves of the recognition rate of the proposed descriptor by different types of SVM with different γ value on the database FVC2002 DB2_a

As we know from the section 3.3, the linear SVM has no parameters, the Radial-basis SVM has only one paramter γ, the Polynominal SVM has three parameters of c, γ, Degree and

the Sigmoid SVM has two paramters of c, γ . For evaluating the recognition rate performance of the proposed tessellated IM based descriptor with different types of SVM, Figure 6 describes the curves of the recognition rate of the proposed descriptor by different types of SVM with different γ value on the database FVC2002 DB2_a. In our experiments, the parmeters of c and Degree are fixed and determined by experiments, and the egienvalues element is 50. From the figure, we can see that the recognition rates of the proposed descriptor of all nonlinear types of SVM are growing up with the γ value, and the proposed descriptor can achieve high recognition rates with the nonlinear types of SVM.

Figure 7 shows the curves of the recognition rate of the proposed descriptor by different γ value of the radial-basis SVM with different PCA egienvalues elements on the database FVC2002 DB2_a. From the figure, we can see that the recognition rate is growing up with the γ value of the Radial-basis SVM. And the descriptor with different egienvalue elements PCA has different recognition rate, with small egienvalue(such as 10) the recognition rate is lower than the PCA with large egienvalue (such as 20) under the same γ value, and the best recognition rate achieves by the egienvalue element equals 50. However, all the recognition rate of the descriptor with PCA may have better performances comparing with the descriptor without PCA.

4.2 Comparing with other descriptors

The performances of several descriptors aimed at evaluating the usefulness of our descriptor were compared; all the descriptors were based on the two-stage enhanced image:

1. Gabor filters based, a descriptor using both minutiae and a ridge feature map with eight directions for fingerprint matching according to the method of Ross et al. (2003), and the same parameters as their paper are used;
2. DCT based, a descriptor using DCT features for fingerprint matching according to the method of Amornraksa & Tachaphetpiboon (2006), and the same parameters as their paper are used;
3. WFMT based, a descriptor using WFMT features for fingerprint matching according to the method of Jin et al. (2004), and the same parameters as their paper are used;
4. LBP based, a descriptor using the invariant local binary patterns features (P = 8; R=1; n=10) according to the method of Nanni & Lumini (2008).
5. Tessellated IM based, the 64×64 pixels ROI was tessellated into 16 rectangular cells with each cell had a size of 16×16 pixels and matching with SVM.

In our experiment, to compute the FAR and the FRR, the genuine match and impostor match were performed on the four sub-databases of FVC2002 database. We divided each database into a training set and a testing set using a 25% jackknife method. Six out of eight fingerprints from each person were chosen for training and the remaining two for testing. For a database, therefore, 600 patterns are used for training, and 200 for testing. For genuine match, each fingerprint of each person is compared with other fingerprints of the same person. And for impostor match, each test fingerprint is compared with the fingerprints belonged to other persons. Since there are 200 test patterns for an experiment, the number of matches for genuine and impostor are 6×200=1200 and 99×200=19800 for each database. The same experiments are repeated four times by selecting different fingerprints for training and testing, and then the average of four experimental results becomes the final performance.
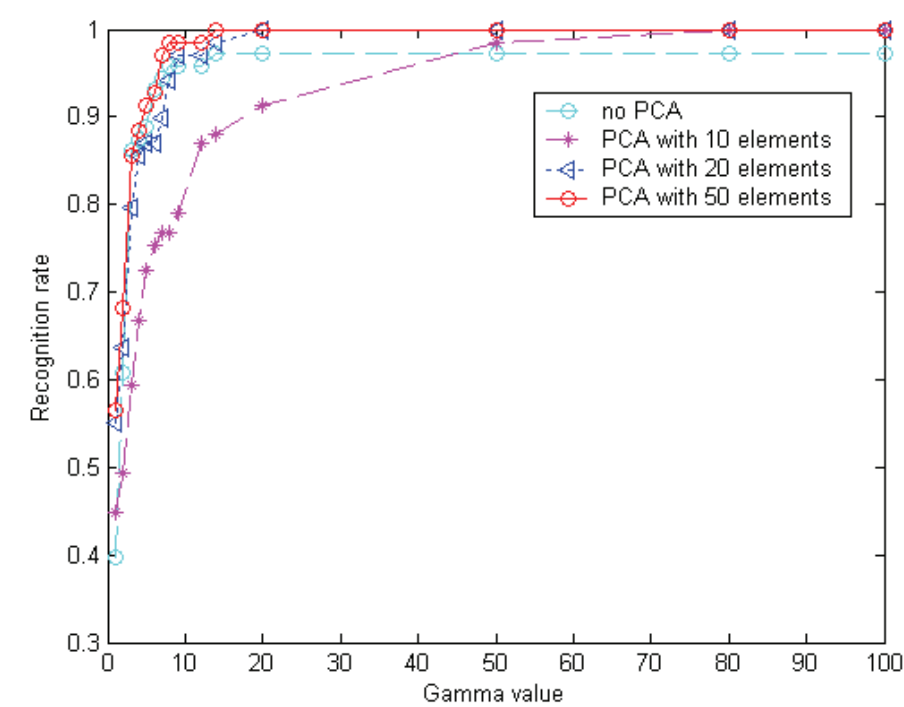
Fig. 7. The curves of the recognition rate of the proposed descriptor by different γ values of the radial-basis SVM with different PCA egienvalues elements on the database FVC2002 DB2_a
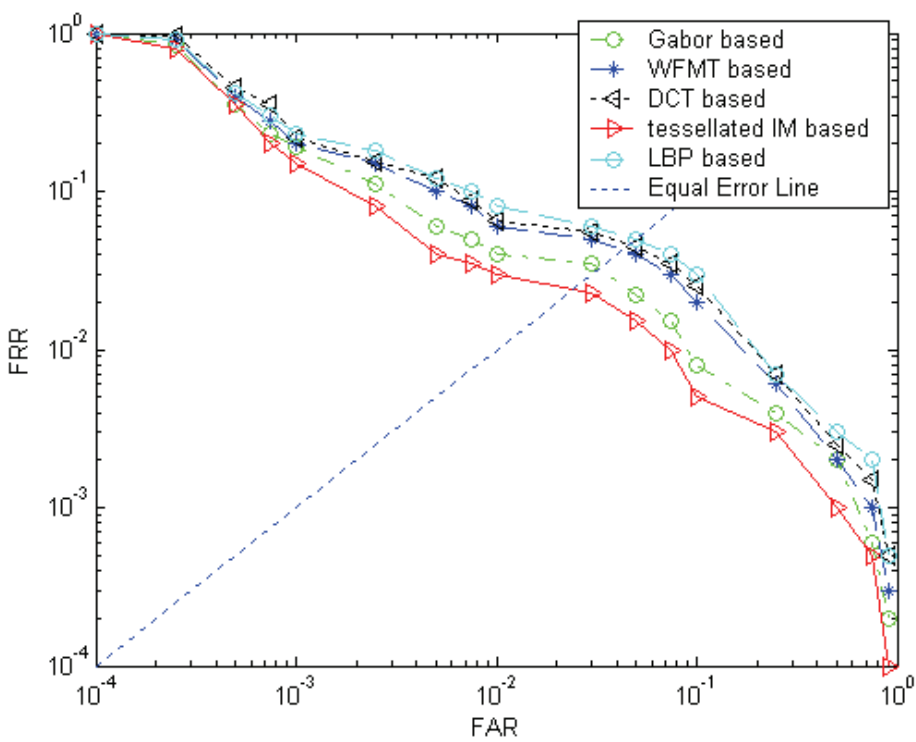

Fig. 8. ROC curves of different methods on database FVC2002 DB2_a

Figure 8 compares the ROC curves of the descriptors of Gabor filters, DCT, WFMT, LBP based with tessellated IM based descriptor on the database FVC2002 DB2_a. On database containing most poor quality images such as FVC2002 DB2_a, the FRRs of all the descriptors slowly drop down with respect to their FARs; The ROC curves of the Figure 8 prove the facts. On the other hand, we can see that the ROC curve of tessellated IM based descriptor (solid line) is below those of the descriptors of Gabor filters, DCT, WFMT, LBP based (dashed lines), which means that tessellated IM based descriptor outperforms the compared descriptors.

And Table 4 illustrates the EER (%) performances of the descriptors of Gabor filters based, DCT based, WFMT based and LBP based with Tessellated IM based over the databases of FVC2002. From the table, we can see that the Tessellated IM based descriptor has the best of results with an average EER of 2.36% over the four sub-databases of FVC2002, while those of the descriptors of Gabor filters, DCT, WFMT, LBP based are 4.17%, 5.68%,4.66%,5.97%, respectively.

	DB1_a	DB2_a	DB3_a	DB4_a	Average
Gabor filters based	1.87	3.98	4.64	6.21	4.17
DCT based	2.96	5.42	6.79	7.53	5.68
WFMT based	2.43	4.41	5.18	6.62	4.66
LBP based	3.21	5.62	6.82	8.23	5.97
Tessellated IM based	1.42	2.23	2.48	3.31	2.36

Table 4. EER(%) performance of the descriptors of Gabor filters, DCT, WFMT , LBP based and tessellated IM based over the databases of FVC2002

5. Conclusion

In this chapter, we emphases on the introduction of the designing approaches and implementing technologies for non-minutiae based fingerprint descriptors. We firstly review some classical and state of the art fingerprint descriptor, analyze their feature extraction, alignment method and matching methods, and propose a non-minutiae based fingerprint descriptor by using tessellated IM features with a feature selection of PCA and a SVM classifier. The scheme consists of other three important steps after the pervious pre-processing: feature vector construction, feature selection with PCA, and matching with a SVM. Experimental results show that our proposed descriptor has better performances of matching accuracy comparing to other prominent descriptors on public databases.

The contributions of this chapter are that we analyze and summarize some classical and state of the art non-minutiae based descriptors and propose a new improved one with tessellated IM features, feature selection by PCA and intelligent SVM to represent fingerprint image in order to effectively handle various input conditions. Further works need to be explored for robustness and reliability of the system.

6. Acknowledgment

7. References

Amornraksa, T. ; Tachaphetpiboon, S. (2006). Fingerprint recognition using DCT features, *Electron. Lett.*, 42(9), pp. 522–523

Benhammadi, F. ;Amirouche, M.N. ;Hentous, H. ; Beghdad, K.B ; Aissani, M. (2007). Fingerprint matching from minutiae texture maps, *Pattern Recognition*,40(1), pp.189-197

Cappelli, R.; Ferrara, M.; Maltoni, D.(2011). Minutia Cylinder-Code: A New Representation and Matching Technique for Fingerprint Recognition, *IEEE Transactions on Pattern Analysis and Machine Intelligence*, 32(12), pp: 2128 - 2141

Dalal, N.,; Triggs, B. (2005). Histograms of oriented gradients for human detection. *In Proceedings of the ninth European conference on computer vision*, San Diego,CA

Fausett, L. (1994), *Fundamentals of Neural Networks architecture, algorithm and application* (Prentice Hall) 289-304

Gonzalez, R. C. ; Woods, R E.(2002), *Digital Image Processing (second edition),* Prentice Hall, pp. 672-675

Hao, P.Y. ; Chiang, J.H. ; Lin Y.H. (2007). A new maximal-margin spherical-structured multi-class support vector machine. *Applied Intelligence,* 30(2), pp.98-111

He, X. ; Tian, J. ; Li, L. ; He, Y ; Yang X.(2007). Modeling and Analysis of Local Comprehensive Minutia Relation for Fingerprint Matching, *IEEE Transactions on Systems, Man, and Cybernetics, Part B: Cybernetics*, 4, 37(5), pp.1204-1211

Hu, M.K.(1962). Visual pattern recognition by moment invariants, *IRE Trans. Info. Theory.* IT-8,pp. 179-187

Jain, A. K.; Hong, L. ; Bolle, R. (1997a). On-line fingerprint verification, *IEEE Trans.Pattern Analysis and Machine Intelligence*, 19, pp. 302–313

Jain, A.K. ; Hong, L. ; Pankanti, S. ; Bolle, R. (1997b) .An identity-authentication system using fingerprints, *Proc. IEEE*, 85(9) pp. 1365-1388

Jain, A.K. ; Prabhakar, S. ; Hong, L. ; Pankanti, S. (2000). Filterbank-based fingerprint matching, *IEEE Trans. Image Processing*,9(5),pp. 846-859

Jiang, X. ; Yau, W.(2000). Fingerprint minutiae matching based on the local and global structures, *International Conference on Pattern Recognition*, pp. 1038–1041

Jin, A.T.B. ; Ling, D.N.C. ; Song, O.T. (2004). An efficient fingerprint verification system using integrated wavelet and Fourier-Mellin invariant transform, *Image and Vision Computing,* 22(6),pp. 503-513

John, S.T. ; Nello, C. (2000), *Support Vector Machines and other kernel-based learning methods,* Cambridge University Press

Kenneth, N. ; Josef, B. (2003). Localization of corresponding points in fingerprints by complex filtering, *Pattern Recognition Letters,* 24 ,pp.2135-2144

Liu, J. ; Huang, Z. ; Chan K.(2000). Direct minutiae extraction from gray-level fingerprint image by relationship examination, *Int. Conf.. Image Processing*, 2,pp. 427-430

Maio, D. ; Maltoni, D.(1997). Direct gray scale minutia detection in fingerprints, *IEEE Trans.Pattern Analysis and Machine Intelligence*,19(1), pp. 27-39

Maio, D. ; Maltoni, D. ; Cappelli, R. ; Wayman, J.L. ; Jain, A.K.(2002). FVC2002: Second Fingerprint Verification Competition, *Proc. Internationl Conference on Pattern Recognition,*(3), pp.811-814

Maltoni, D. ;Maio, D. ;Jain, A.K. ; Prabhakar S. (2003). *Handbook of Fingerprint Recognition*, Springer, Berlin, pp.135-137

Nagaty, K.A.(2005). An adaptive hybrid energy-based fingerprint matching technique, *Image and Vision Computing,* 23,pp.491-500

Nanni, L. ; Lumini, A. (2007). A hybrid wavelet-based fingerprint matcher, *Pattern Recognition*, 40(11),pp. 3146-3151

Nanni, L. ; Lumini, A. (2008). Local Binary Patterns for a hybrid fingerprint matcher, *Pattern Recognition,* 41(11), pp.3461-3466

Nanni, L. ; Lumini, A.(2009). Descriptors for image-based fingerprint matchers, *Expert Systems With Applications,* 36(10), pp.12414-12422

Ojala, T., Pietikainen, M., & Maeenpaa, T. (2002). Multiresolution gray-scale androtation invariant texture classification with local binary patterns. *IEEE Transactions on Pattern Analysis and Machine Intelligence,* 24(7), pp.971–987.

Papoulis, A. (1991). *Probablity, random variables and stochastic processes*, Boston: McGraw-Hill.

Ratha, N. K. ; Karu, K. ; Chen, S. ; Jain, A. K.(1996). A real-time matching system for large fingerprint databases, *IEEE Transactions on Pattern Analysis and Machine Intelligence,* 18(8), pp.799–813

Ross, A., Jain, A.K., Reisman, J.(2003). A hybrid fingerprint matcher, *Pattern Recognition,* 36(7), pp. 1661-1673

Sha, L.F. ; Zhao F. ; Tang X.O.(2003). Improved fingercode for filterbank-based fingerprint matching, *Int. Conf. Image Processing*, pp.895-898

Tico, M. ; Kuosmanen, P. ; Saarinen, J. (2001) . Wavelet domain features for fingerprint recognition, *Electron. Lett.*, 37(1), pp. 21–22

Yang, J.C. ; Yoon, S. ; Park, D.S. (2006). Applying learning vector quantization neural network for fingerprint matching, *Lecture Notes in Artificial Intelligence (LNAI 4304)* (Springer, Berlin) , pp.500-509

Yang, J.C. ; Park, D. S. (2008a). A fingerprint verification algorithm using tessellated invariant moment features, *Neurocomputing,* 71(10-12), pp.1939-1946

Yang, J.C. ; Park, D. S. (2008b). Fingerprint Verification Based on Invariant Moment Features and Nonlinear BPNN, *International Journal of Control, Automation, and Systems,* 6(6), pp.800-808

Yang, J.C. ; Park, D.S. ; Hitchcock, R. (2008c). Effective Enhancement of Low-Quality Fingerprints with Local Ridge Compensation, *IEICE Electronics Express,* 5(23), pp.1002–1009
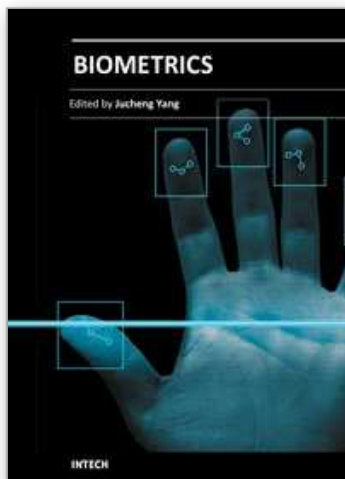
Biometrics

Edited by Dr. Jucheng Yang

Biometrics uses methods for unique recognition of humans based upon one or more intrinsic physical or behavioral traits. In computer science, particularly, biometrics is used as a form of identity access management and access control. It is also used to identify individuals in groups that are under surveillance. The book consists of 13 chapters, each focusing on a certain aspect of the problem. The book chapters are divided into three sections: physical biometrics, behavioral biometrics and medical biometrics. The key objective of the book is to provide comprehensive reference and text on human authentication and people identity verification from both physiological, behavioural and other points of view. It aims to publish new insights into current innovations in computer systems and technology for biometrics development and its applications. The book was reviewed by the editor Dr. Jucheng Yang, and many of the guest editors, such as Dr. Girija Chetty, Dr. Norman Poh, Dr. Loris Nanni, Dr. Jianjiang Feng, Dr. Dongsun Park, Dr. Sook Yoon and so on, who also made a significant contribution to the book.

How to reference

In order to correctly reference this scholarly work, feel free to copy and paste the following:

INTECH
open science | open minds